ASCE Geotechnical Special Publication honoring Dr. John H. Schmertmann.
FROM RESEARCH TO PRACTICE IN GEOTECHNICAL ENGINEERING
GSP No. 170, 2008

Geo-Institute Meeting in New Orleans March 9 to 12, 2008

In Situ Tests by Seismic Dilatometer (SDMT)

Silvano Marchetti[1], Paola Monaco[2], Gianfranco Totani[3] and Diego Marchetti[4]

[1]Professor, University of L'Aquila, Faculty of Engineering, DISAT, 67040 Monteluco di Roio, L'Aquila, Italy; marchetti@flashnet.it
[2]Assistant Professor, University of L'Aquila, Faculty of Engineering, DISAT, 67040 Monteluco di Roio, L'Aquila, Italy; p.monaco@ing.univaq.it
[3]Associate Professor, University of L'Aquila, Faculty of Engineering, DISAT, 67040 Monteluco di Roio, L'Aquila, Italy; totani@ing.univaq.it
[4]Studio Prof. Marchetti, Via Bracciano 38, 00189 Roma, Italy; diego@marchetti-dmt.it

ABSTRACT: The seismic dilatometer (SDMT) is the combination of the standard flat dilatometer (DMT) with a seismic module for measuring the shear wave velocity V_S. This paper summarizes the experience gained from SDMT tests performed at 34 sites. In particular the paper presents an overview of the SDMT equipment, comparisons of V_S measured by SDMT and by other methods, interrelationships G_0, E_D, M_{DMT} based on 2000 data points and a selection of significant SDMT results and related comments. The paper also illustrates the major issues of present research on use and applications of the SDMT, mostly focused on the development of methods for deriving the in situ G-γ decay curves and for evaluating the liquefaction resistance of sands based on SDMT results.

KEYWORDS: Seismic Dilatometer SDMT, Flat Dilatometer DMT, Shear Wave Velocity V_S, G-γ Curves, Working Strain Modulus, Liquefaction

INTRODUCTION

The seismic dilatometer (SDMT) is the combination of the traditional "mechanical" Flat Dilatometer (DMT) introduced by Marchetti (1980) with a seismic module placed above the DMT blade. The SDMT module is a probe outfitted with two receivers, spaced 0.5 m, for measuring the shear wave velocity V_S. From V_S the maximum shear modulus G_0 may be determined using the theory of elasticity.

Motivations of the combined probe:

– V_S (and G_0) are at the base of any seismic analysis.
– The G-γ decay curves are an increasingly requested input in seismic analyses and in general in non linear analyses.
– Increasing demand for liquefiability evaluations.
– Seismic site classification using directly V_S rather than N_{SPT} or c_u.

– Availability of the usual DMT results (e.g. constrained modulus M_{DMT}) for current design applications (e.g. conventional settlement predictions).

This paper comments on the most significant SDMT results obtained in the period 2004-2007 at 34 sites.

Information on the mechanical DMT, not described in this paper, can be found in the comprehensive report by the ISSMGE Technical Committee TC16 (2001).

THE SEISMIC DILATOMETER (SDMT)

The seismic dilatometer (SDMT) is the combination of the standard DMT equipment with a seismic module for measuring the shear wave velocity V_S.

The test is conceptually similar to the seismic cone SCPT. First introduced by Hepton (1988), the SDMT was subsequently improved at Georgia Tech, Atlanta, USA (Martin and Mayne 1997, 1998; Mayne et al. 1999). A new SDMT system (Fig. 1) has been recently developed in Italy. The seismic module (Fig. 1a) is a cylindrical element placed above the DMT blade, equipped with two receivers, spaced 0.5 m. The signal is amplified and digitized at depth. The *true-interval* test configuration with two receivers avoids possible inaccuracy in the determination of the "zero time" at the hammer impact, sometimes observed in the *pseudo-interval* one-receiver configuration. Moreover, the couple of seismograms recorded by the two receivers at a given test depth corresponds to the same hammer blow and not to different blows in sequence, which are not necessarily identical. Hence the repeatability of V_S measurements is considerably improved (observed V_S repeatability ≈ 1-2 %). V_S is obtained (Fig. 1b) as the ratio between the difference in distance between the source and the two receivers (S_2 - S_1) and the delay of the arrival of the impulse from the first to the second receiver (Δt). V_S measurements are obtained every 0.5 m of depth.

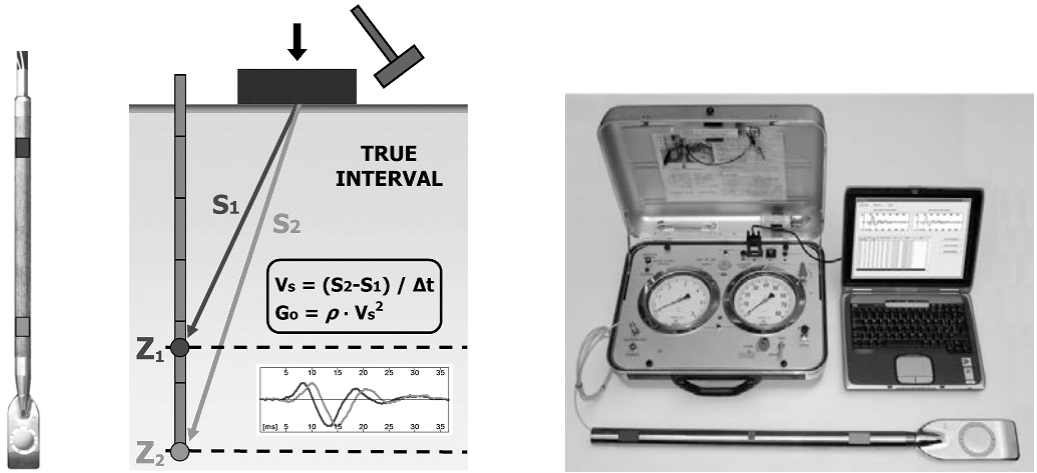

FIG. 1. Seismic Dilatometer: (a) DMT blade and seismic module. (b) Schematic layout of the seismic dilatometer test. (c) Seismic dilatometer equipment.

FIG. 2. Shear wave source at the surface

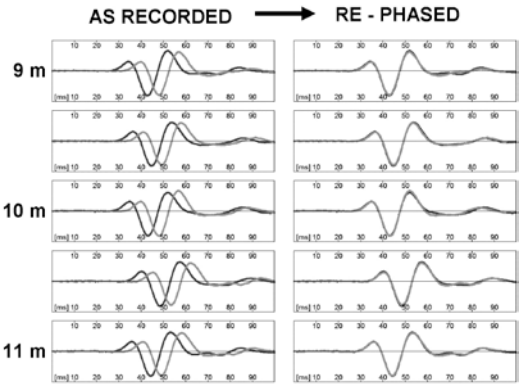

FIG. 3. Example of seismograms obtained by SDMT at the site of Fucino (Italy)

The shear wave source at the surface (Fig. 2) is a pendulum hammer (≈ 10 kg) which hits horizontally a steel rectangular base pressed vertically against the soil (by the weight of the truck) and oriented with its long axis parallel to the axis of the receivers, so that they can offer the highest sensitivity to the generated shear wave.

The determination of the delay from SDMT seismograms, normally carried out using the cross-correlation algorithm, is generally well conditioned being based on the two seismograms – in particular the initial waves – rather than being based on the first arrival time or specific marker points in the seismogram.

Fig. 3 shows an example of seismograms obtained by SDMT at various test depths at the site of Fucino (it is a good practice to plot side-by-side the seismograms as recorded and re-phased according to the calculated delay).

Fig. 4 (Fiumicino) is an example of the typical graphical format of the SDMT output. Such output displays the profile of V_S as well as the profiles of four basic

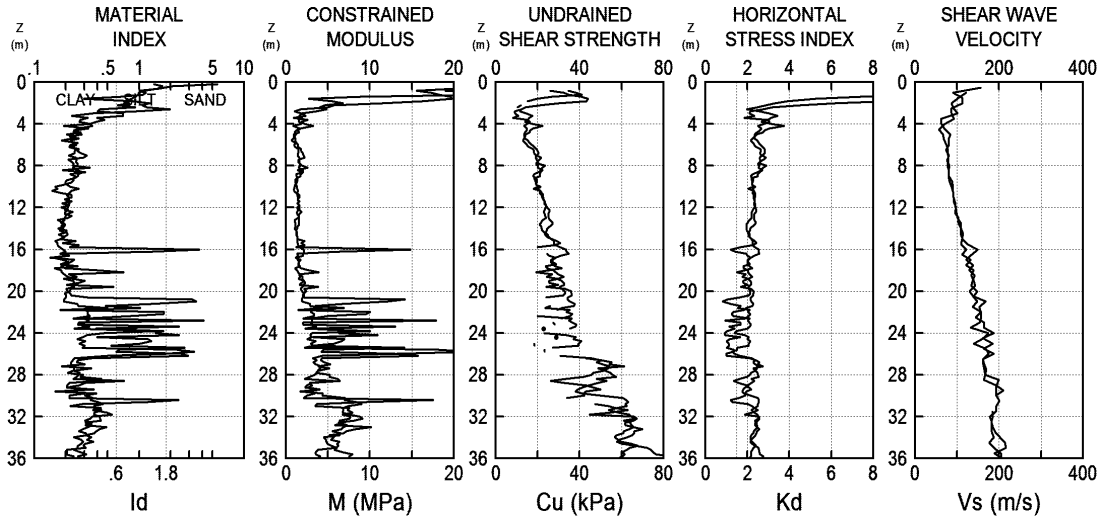

FIG. 4. SDMT profiles at the site of Fiumicino (Italy)

TABLE 1. Example of repeatability of V_S measurements by SDMT (Zelazny Most Tailing Dam, Poland)

Z [m]	V_S [m/s]	V_S values [m/s] corresponding to different hammer blows at each depth Z	Coefficient of variation [%]
7.00	179	178,178,180,180,180,179,179,180,180,180	0.50
7.50	231	234,232,232,230,229,231,232,229,230	0.68
8.00	225	227,225,224,225,225,225,226,226,225,224,224	0.40
8.50	276	276,276,280,273,275,273,271,273,287,281	1.68
9.00	296	291,286,301,292,296,288,301,300,304,303	2.09
9.50	248	244,251,250,247,250,249,250,249,242,248	1.11
10.00	292	292,289,290,293,289,292,289,292,296,295,293	0.79
10.50	320	321,323,320,325,323,325,316,314,308,321	1.61
11.00	291	293,291,293,291,291,290,290,291,290,290	0.38
11.50	321	324,320,320,322,320,322,319,319,320,320	0.48
12.00	309	311,307,311,309,309,311,309,309,307,311	0.50
12.50	286	287,285,285,285,287,285,285,287,287,287	0.35
13.00	265	265,265,265,264,265,265,265,266,265,266,264	0.24
13.50	280	287,276,279,276,276,276,294,275,278,279	2.08
14.00	312	313,312,312,322,310,312,310,310,310,312	1.10
14.50	298	301,298,299,299,298,296,299,298,299,298	0.44
15.00	309	307,309,307,309,309,309,309,309,309,309	0.29

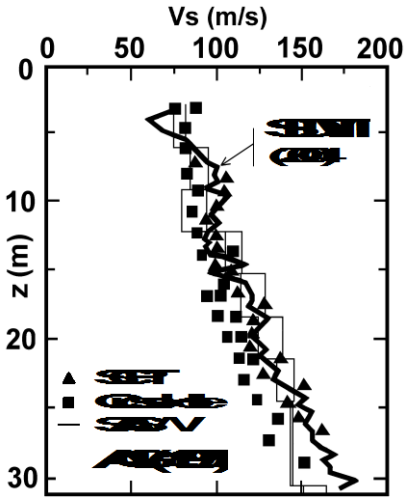

FIG. 5. Comparison of V_S profiles obtained by SDMT and by SCPT, Cross-Hole and SASW (AGI 1991) at the research site of Fucino (Italy)

DMT parameters – the material index I_D (soil type), the constrained modulus M, the undrained shear strength c_u and the horizontal stress index K_D (related to OCR) – obtained using current DMT correlations. It may be noted from Fig. 4 that the repeatability of the V_S profile is very high, similar to the repeatability of the other DMT parameters, if not better.

Table 1 shows an example of another kind of repeatability of V_S by SDMT (Zelazny Most Tailing Dam, Poland). Each V_S value at a given test depth corresponds to a different hammer blow. The coefficient of variation of V_S is in the range 1-2 %.

Such repeatability is more than adequate for normal engineering needs. However, especially in earthquake geotechnical engineering, where the design is increasingly based on the acceptability of the permanent displacements, accurate V_S (and G_0) estimates are a necessary prerequisite for correctly predicting such displacements.

V_S measurements by SDMT have been validated by comparison with V_S measurements obtained by other in situ seismic tests at various research sites. As an example Fig. 5 shows V_S comparisons at the research site of Fucino, Italy (NC cemented clay), extensively investigated at the end of the '80s. The profile of V_S obtained by SDMT in 2004 (Fig. 5) is in quite good agreement with V_S profiles obtained by SCPT, Cross-Hole and SASW in previous investigations (AGI 1991). Similar favourable comparisons are reported by various Authors, e.g. by Hepton (1988), McGillivray and Mayne (2004) and Młynarek et al. (2006).

INTERRELATIONSHIPS BETWEEN EXPERIMENTAL G_0, E_D, M_{DMT}

The experimental diagrams presented in this section have been constructed using same-depth G_0, E_D, M_{DMT} values determined by SDMT at 34 different sites, in a

variety of soil types. The majority of the sites are in Italy, others are in Spain, Poland, Belgium and USA.

SDMT generates plentiful data points because each sounding routinely provides profiles of G_0, E_D, M_{DMT}. Of the over 2000 data points available, only 800 high quality data points have been considered, relative to "uniform" one-m soil intervals where log I_D, K_D, E_D, M_{DMT}, V_S all differ less than 30 % from their average – used then to plot the data points – to insure a proper match of the data.

The DMT parameters have been calculated with the usual DMT interpretation formulae as in Marchetti (1980) or Table 1 in TC16 (2001).

Diagrams of the Ratio G_0/E_D

The ratio G_0/E_D are plotted versus K_D (Fig. 6a) and I_D (Fig. 6b). It can be seen that data points tend to group according to their I_D and K_D. From Fig. 6, if I_D and K_D are available, rough estimates of G_0 can be made from E_D, in absence of direct G_0 measurements.

Recognizable trends in Fig. 6 are: G_0/E_D is mostly in the range 1.5 to 3 in sand, 2.5 to 13 in silt, 3 to 25 in clay. The widest range and the maximum variability of G_0/E_D are found in clay. For all soils G_0/E_D decreases as K_D (related to OCR) increases.

Diagrams of the Ratio G_0/M_{DMT}

The ratio G_0/M_{DMT} are plotted versus K_D (Fig. 7a) and I_D (Fig. 7b). The diagrams indicate a wide range of the ratio G_0/M_{DMT} (≈ 0.5 to 25 for all soils), hence the unfeasibility of estimating the operative modulus M from G_0 by dividing G_0 for a fixed number. Again the data points tend to group according to their I_D and K_D. It can be seen that G_0/M_{DMT} is strongly dependent on (at least) both soil type and stress history. Hence the use of only one parameter (e.g. c_u in cohesive soils) as an estimate for V_S (or G_0) for the seismic soil classification appears problematic.

Recognizable trends in Fig. 7 are: G_0/M_{DMT} is mostly in the range 0.5 to 3 in sand, 1 to 10 in silt, 1 to 20 in clay. The widest range and the maximum variability of G_0/M_{DMT} are found in clay. For all soils G_0/M_{DMT} decreases as K_D (related to OCR) increases.

If I_D and K_D are available, Fig. 7, where the dispersion is slightly less than in Fig. 6, is to be preferred to Fig. 6 to obtain rough estimates of the ratio G_0/M, i.e. G_0 from M or M from G_0, when only one of them is available.

Diagrams of the Ratio G_{DMT}/G_0

Fig. 8 shows the same experimental information as in Figures 6 and 7, but involves the additional modulus G_{DMT} derived from M_{DMT} using the formula of linear elasticity:

$$G = M / [2\ (1-\nu) / (1-2\nu)] \qquad (1)$$

For ν = 0.15, 0.20 and 0.25, the denominator in Eq. 1 would be 2.43, 2.67 and 3

respectively. For the conversion, the denominator 2.67 has been retained, i.e.:

$$G_{DMT} = M_{DMT} / 2.67 \quad (2)$$

All the G_{DMT} have been derived from M_{DMT} using Eq. 2, then the ratios G_{DMT}/G_0 have been calculated too and plotted versus K_D (Fig. 8a) and I_D (Fig. 8b).

The reason of constructing Fig. 8 is the following. The ratio G/G_0 is the usual ordinate of the normalized G-γ decay curve and has the meaning of a strain decay factor. Since M_{DMT} is a *working strain modulus* one might hypothesize that G_{DMT} is a *working strain shear modulus* too, in which case G_{DMT}/G_0 could be regarded as the shear modulus decay factor at *working strains*.

It is emphasized that, at this stage, the legitimacy of using linear elasticity for deriving G_{DMT} from M_{DMT} (Eq. 2) and the assumption that G_{DMT} is a *working strain shear modulus* are only working hypotheses, likely more difficult to investigate than verifying that M_{DMT} is a *working strain constrained modulus* (the matter is discussed later in the paper). The very designation *working strain shear modulus* (or operative shear modulus) requires clarification. Anyway, if the above hypotheses were acceptable, Fig. 8 could provide, if I_D and K_D are known, rough estimates of the decay factor at *working strains*. If complete SDMT are available, then said rough estimates could be skipped and the decay factor could be obtained directly as the ratio between G_{DMT} from Eq. 2 and G_0.

Trends emerging from Fig. 8 are: (a) The G decay in sands is much less than in silts and clays. (b) The silt and clay decay curves are very similar. (c) For all soils the decay is maximum in the NC or lightly OC region (low K_D).

Fig. 7a and Fig. 8a are reproduced in a more readable format in Fig. 9 and Fig. 10 respectively, where the data points relative to clay, silt and sand have been plotted separately. Best fit equations are indicated for each of the six diagrams.

IN SITU G-γ DECAY CURVES BY SDMT

SDMT provides routinely at each depth, besides a *small strain modulus* (G_0 from V_S), also a *working strain modulus* (M_{DMT}). These two moduli could possibly be of help when selecting the G-γ curves. Such potentiality is heavily founded on the basic premise that M_{DMT} is a reasonable estimate of the operative *working strain modulus*. It is therefore considered appropriate to recall here the presently available evidence.

M_{DMT} as an Operative or Working Strain Modulus

The terms Operative Modulus and Working Strain Modulus are considered synonyms in this paper and are used interchangeably. They are defined as those moduli that, introduced into the linear elasticity formulae, provide reasonable estimates of the settlements under a shallow foundation (say for a safety factor Fs ≈ 2.5 to 3.5).

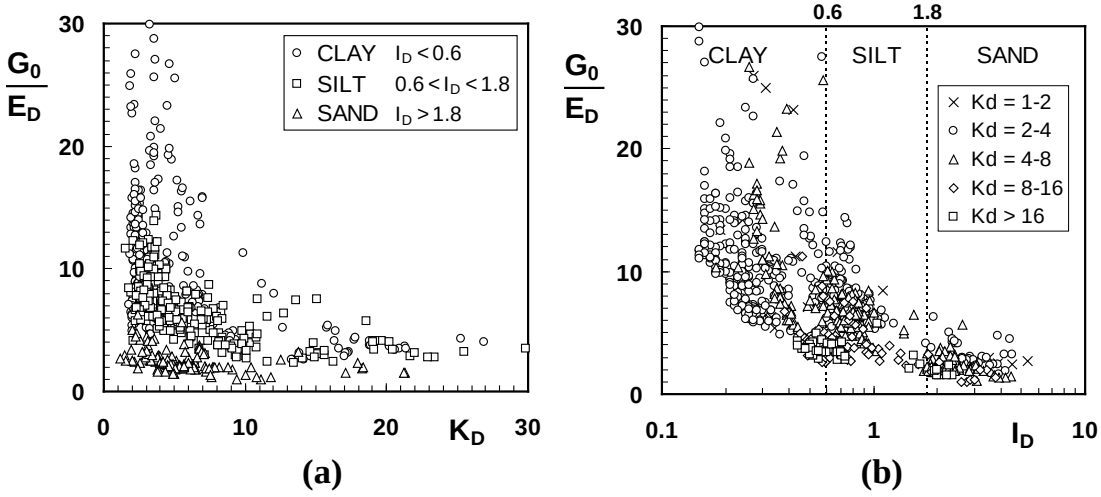

FIG. 6. Ratio G_0/E_D vs. K_D and I_D

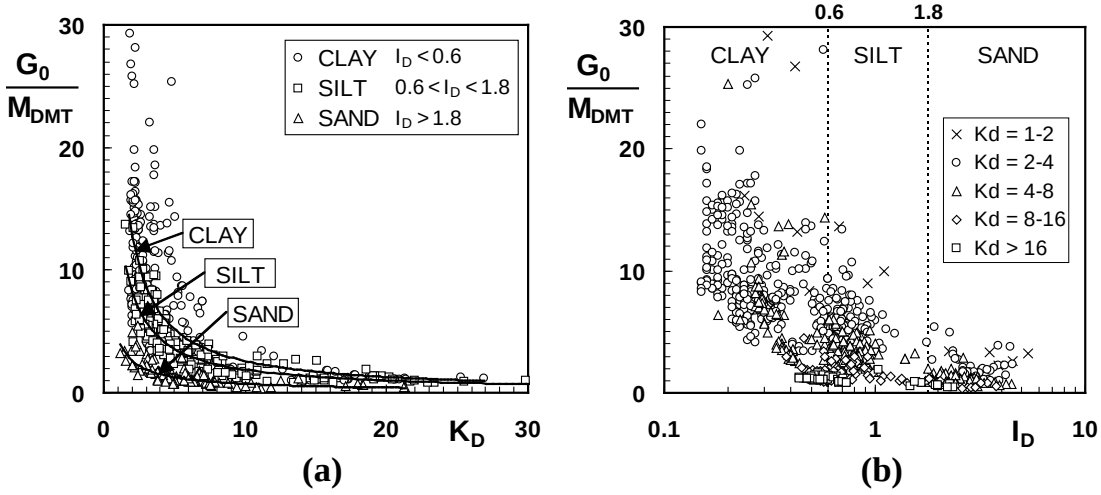

FIG. 7. Ratio G_0/M_{DMT} vs. K_D and I_D

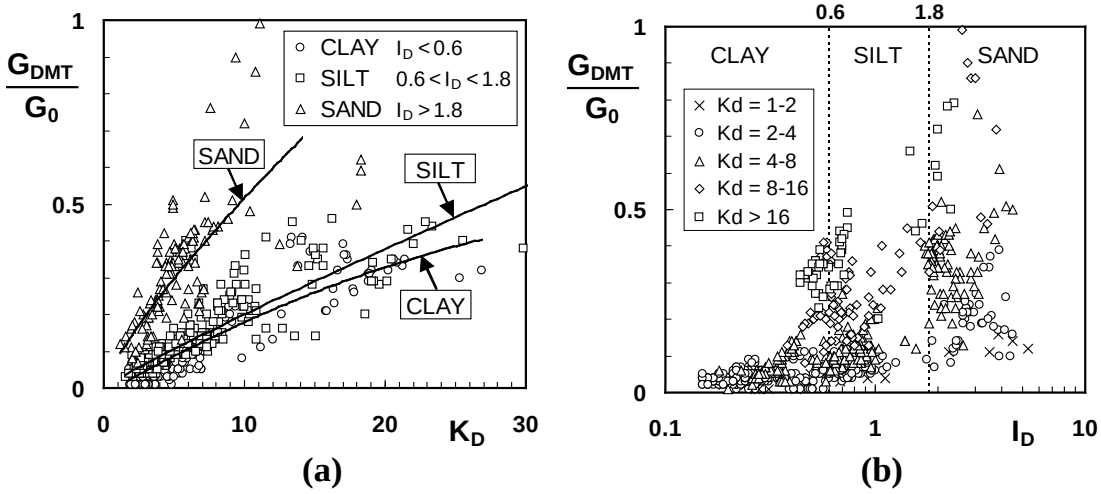

FIG. 8. Decay ratio G_{DMT}/G_0 vs. K_D and I_D

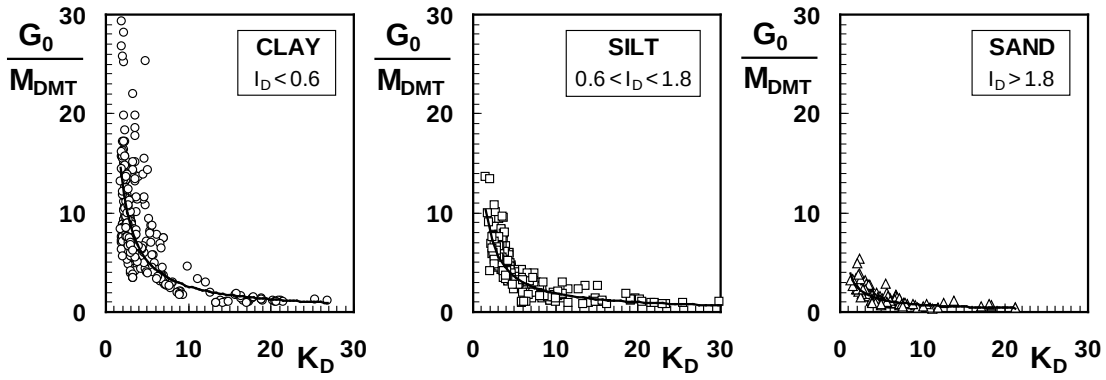

FIG. 9. Ratio G_0/M_{DMT} vs. K_D for clay, silt and sand

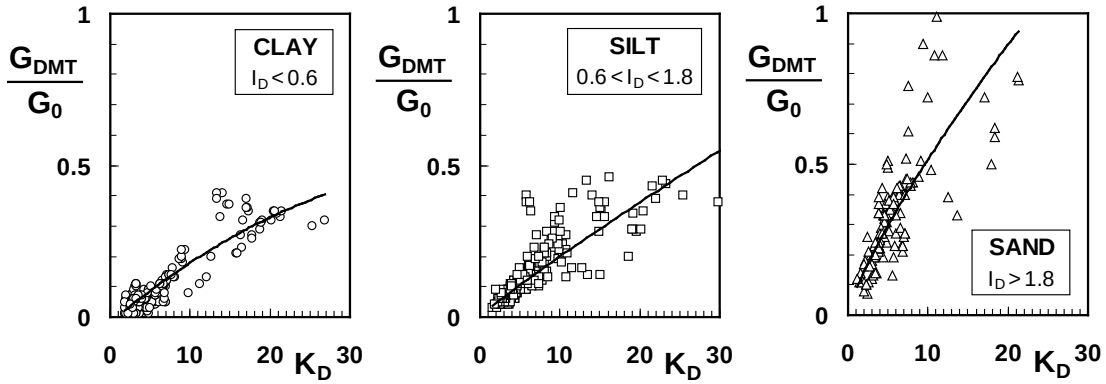

FIG. 10. Decay ratio G_{DMT}/G_0 vs. K_D for clay, silt and sand

Comparisons of Surface Settlements

Schmertmann (1986) reported 16 case histories at various locations and for various soil types, with measured settlements ranging from 3 to 2850 mm. In most cases settlements from DMT were calculated using the Ordinary 1-D Method. The average ratio DMT-calculated/observed settlement was 1.18, with the value of the ratio mostly in the range 0.7 to 1.3 and a standard deviation of 0.38.

Monaco et al. (2006) reviewed numerous other real-life well documented comparisons of DMT-predicted versus measured settlements. The average ratio DMT-calculated/observed settlement for all cases reviewed by Monaco et al. (2006) is ≈ 1.3, with an observed settlement within ± 50 % from the DMT-predicted settlement.

The above settlements comparisons appear to support the assumption that M_{DMT} is a reasonable estimate of the constrained *working strain modulus*.

Comparisons of Moduli

Even more direct, but rarely available, are data comparing M_{DMT} with moduli back-figured from local vertical strain measurements.

In 2002 a major research project, funded by the Italian Ministry of University and Scientific Research and by Consorzio Venezia Nuova, was undertaken by a consortium of three Italian Universities (Padova, Bologna and L'Aquila).

A full-scale cylindrical heavily instrumented test embankment (40 m diameter, 6.7 m height, applied load 104 kPa – Fig. 11a) was constructed at the site of Venezia-Treporti, typical of the highly stratified, predominantly silty deposits of the Venezia lagoon (Fig. 11b). The loading history, the progression of the settlements and the drainage conditions – practically fully drained – are shown in Fig. 11c.

A specific aim of the research was to obtain a profile of the observed 1-D operative modulus *M* under the center of the embankment. For this purpose a high precision sliding micrometer was used to accurately measure the *local* vertical strain ε_v at 1 m depth intervals.

M values were back-calculated from local vertical strains ε_v in each 1 m soil layer as $M = \Delta\sigma_v / \varepsilon_v$, with vertical stress increments $\Delta\sigma_v$ calculated at the mid-height of each layer by linear elasticity formulae (approximation considered acceptable in view of the very low ε_h).

Fig. 11d, which is believed to be one of the *most important results* of the Venezia-Treporti research, shows an overall satisfactory agreement between M_{DMT} and moduli back-figured from the test embankment performance, also considering the marked soil heterogeneity. Fig. 11e compares the observed versus DMT-predicted settlements at each depth. Again the agreement is rather satisfactory, considering that the DMT predicted settlements were calculated using the simple linear 1-D conventional approach $s = \Sigma\,(\Delta\sigma_v / M_{DMT})\,\Delta H$, where $\Delta\sigma_v$ is calculated by Boussinesq linear elasticity formulae.

As to the surface settlements, the total settlement measured under the center of the embankment at the end of construction (180 days) was ≈ 36 cm (Fig. 11c). The settlement predicted by M_{DMT} using the 1-D approach (before knowing the results) was 29 cm. Hence the 29 cm predicted by DMT (which does not include secondary) are in good agreement with the 36 cm observed settlement (which includes some secondary during construction).

(Cunha (2004) wondered if it is right to attribute the 7 cm settlement difference (20 %) to secondary or to other causes. The question is legitimate. But in practical circles settlement predictions within a factor of 1.5-2 are often considered satisfactory for normal design. Mayne (2005) reports an SPT-DMT settlement comparison where the SPT prediction was wrong by a factor of 5 (the DMT prediction "was in line with the observed performance"). Factors of 3 or 5 are not unusual. In general, engineering decisions on the foundation type are based on knowing if the foundation will settle 1 mm or 10 mm or 100 mm. While it is desirable to reduce the error factor below 5 or 3, once it is reduced to 1.5 to 1.2, additional efforts may not be worthwhile or even inherently unfruitful due the many uncertainties involved in the definition of the settlement components and in their precise measurement).

(a) Test embankment. Penetrometer truck for testing after construction.

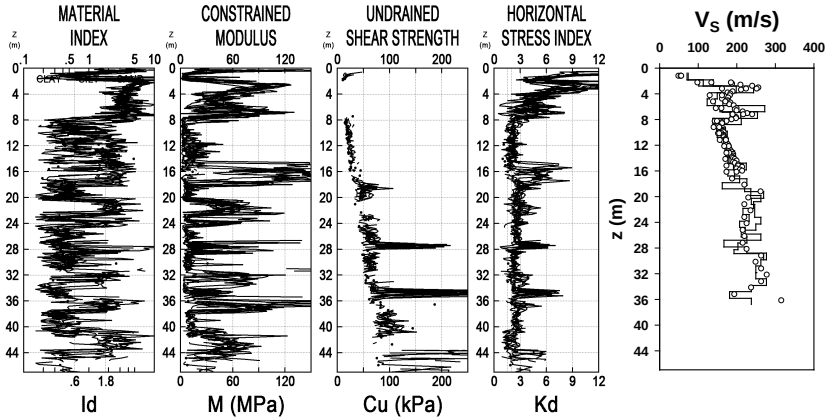

(b) Superimposed profiles of all SDMT data

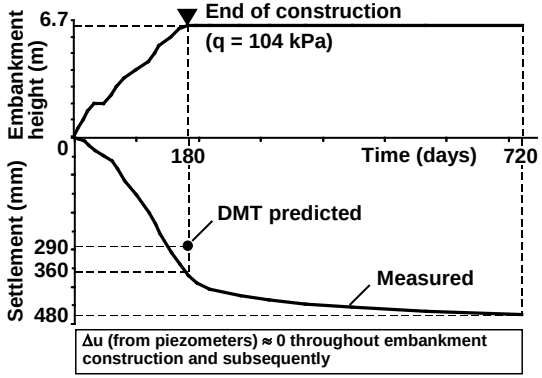

(c) Settlement vs. time at the center of the embankment and comparison of measured vs. DMT-predicted settlements at the end of construction

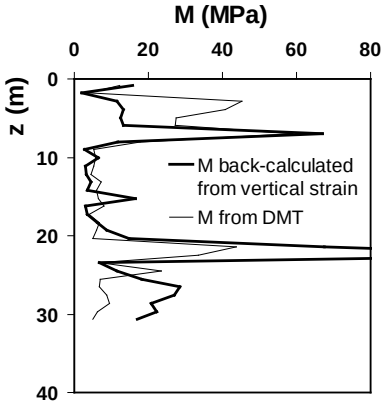

(d) M_{DMT} vs. M back-calculated from local ε_v measured at 1 m depth intervals under the center at the end of construction

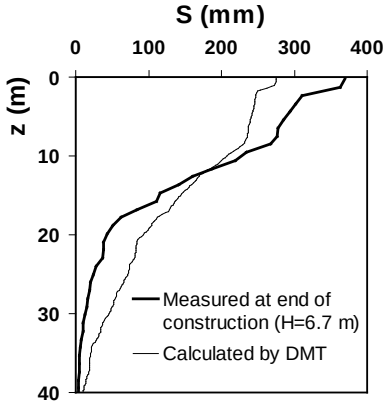

(e) Observed vs. DMT-predicted settlement under the center at the end of construction

FIG. 11. Venezia-Treporti Research Embankment. SDMT profiles. Predicted vs. observed moduli and settlements (Marchetti et al. 2006).

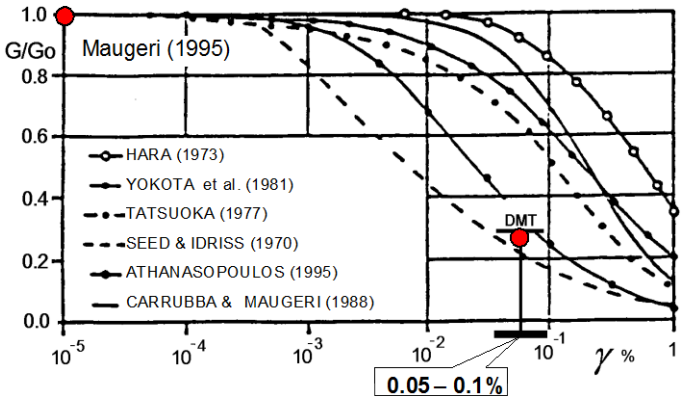

FIG. 12. Tentative method for deriving *G*-γ curves from SDMT

More details on the Venezia-Treporti research can be found in Marchetti et al. (2006), also containing numerous additional bibliographic references.

In conclusion also the Venezia-Treporti case-history supported the assumption that M_{DMT} is a reasonable estimate of the constrained *working strain modulus*.

A note of caution. In OC clays oedometer moduli, even from good quality samples, are generally too low to be taken as operative moduli in situ. As noted by Ladd (1971), quoting Terzaghi-Peck (1964), the compressibility of even good oedometer samples of OC clay may be 2 to 5 times larger than the in situ compressibility. Indeed many engineers feel that the Skempton-Bjerrum reduction factor for settlements in OC clays was prompted by the fact that oedometer-based settlement predictions in OC London clay were systematically too high. Moduli back-figured from local strain measurements are far more realistic and are preferable for calibration or comparison purposes.

Construction of the *G*-γ Curves

Such curves could tentatively be constructed by fitting "reference typical-shape" laboratory curves (see Fig. 12, where G is normalized to G_0) through two points, both obtained by SDMT: (1) the *initial modulus* G_0 from V_S, and (2) a *working strain modulus* G_{DMT} (Eq. 2). To locate the second point it is also necessary to know, at least approximately, the shear strain corresponding to G_{DMT}. Indications by Mayne (2001) locate the DMT moduli at an intermediate level of strain ($\gamma \approx 0.05$-0.1 %) along the *G*-γ curve. Similarly Ishihara (2001) classified the DMT within the group of methods of measurement of soil deformation characteristics involving an intermediate level of strain (0.01-1 %). The above indications, to be supplemented by further investigations, could possibly help develop methods for deriving in situ *G*-γ curves from SDMT.

Lines of research currently under investigation are:

(a) Enter the G_{DMT}/G_0 ratios of Fig. 8 in the vertical axis of "reference typical-shape" *G*-γ curves recommended in the literature for the corresponding soil type. The

range of abscissas of the intersection points with the G-γ curves could possibly help to better define the shear strain corresponding to G_{DMT}.

(b) Develop a procedure for selecting the G-γ curve, among the typical curves recommended in the literature, making use of I_D for choosing the band of curves recommended for the soil type (sand or silt or clay), and K_D (possibly G_0/M_{DMT} too) for selecting one curve in the band.

(c) Evaluate for each of the 800 data points in Figures 6-7-8 the settlement under a simple loading scheme using the simple linear analysis with input M_{DMT} (operation equivalent to converting a DMT investigation into a "virtual" load test). Then calculate the settlement by non linear analyses with G-γ curves having variable rates of decay as input. By trial and error identify the G-γ curve (originating in G_0) producing agreement between the two predicted settlements. Consider such G-γ curve reasonably correct and use it in the development of procedures for selecting the G-γ curves from SDMT data.

DERIVABILITY OF THE OPERATIVE MODULUS *M* FROM G_0

This section discusses the possibility of deriving the operative modulus M by dividing G_0 by a constant.

Fig. 13 (Barcelona airport site) shows that, while the modulus M_{DMT} exhibits a drastic drop at ≈ 12 m depth, at the transition from an upper stiff sand layer to a lower very soft clay layer, V_S shows only a minor decrease. Hence $G_0 = \rho V_S^2$, even considering the power 2, is far from being proportional to the *working strain modulus M*. Similar lack of proportionality, with variations of the ratio G_0/M_{DMT} often of one order of magnitude, has been observed at many sites (including Venezia, Fig. 11d), suggesting that it is next to impossible (at least without local layer-specific correlations) to derive the *working strain modulus* by simply reducing the *small strain modulus* by a fixed percent factor (e.g. 50 %, Simpson 1999).

On the other hand the poor correlability was expected, since at low strains the soil tendency to dilate or contract is not active yet. Such tendency substantially affects the operative modulus M, but does not affect G_0. Said in a different way, M includes some stress history information, G_0 does not (Powell and Butcher 2004).

The high variability of the ratio G_0/M was already noted earlier in Fig. 7. That figure explains that part of the difference in the amount of decrease in the Barcelona M and V_S profiles is due to the transition from sand (where G_0/M_{DMT} is in the range 0.5-3) to clay (where G_0/M_{DMT} is in the range 1-20). Fig. 7 (or the equivalent Fig. 9), entered with I_D and K_D, can provide rough estimates of the ratio, hence M from G_0. However the direct measurements of both M and G_0 are preferable if accurate estimates of these parameters are required.

ESTIMATING OCR IN SAND FOR ADVANCED PREDICTIVE MODELS

Computer programs based on advanced soil models are increasingly used not only by researchers but also by practitioners for everyday design. Hence an important aim of in situ tests is to possibly provide input parameters for such models.

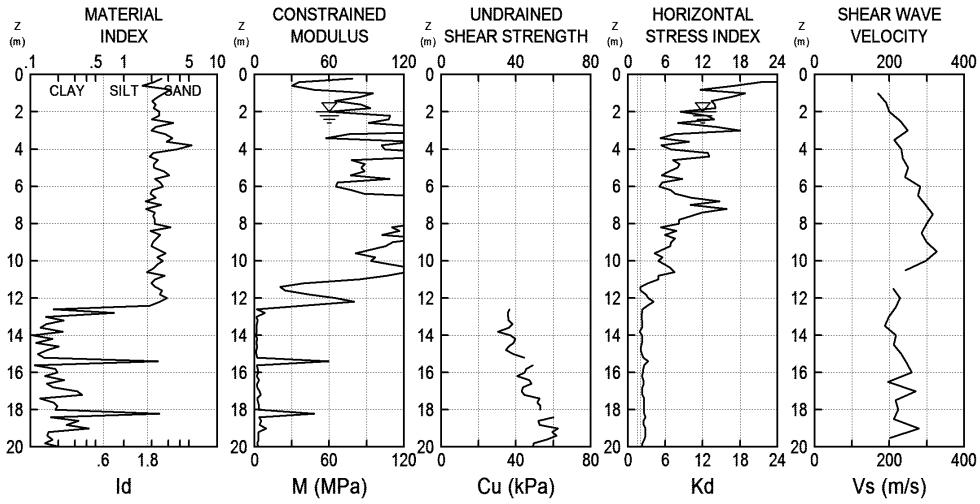

FIG. 13. SDMT profiles at the site of Barcelona – El Prat Airport (Spain)

An input parameter required by many models is OCR. In clays reasonable OCR estimates can be obtained by laboratory samples, or in situ sometimes by the DMT OCR-K_D correlations. In *sands*, however, OCR evaluations are problematic. As today, to the authors' knowledge, one of the least imprecise methods for evaluating OCR in sand by in situ tests is the one suggested by TC16 (2001). Such method consists in evaluating OCR based on the ratio M_{DMT}/q_c (q_c from CPT) using as a guide: M_{DMT}/q_c = 5-10 in NC sands, M_{DMT}/q_c = 12-24 in OC sands. The basis of such ratios is explained in TC16 (2001). In essence: when imparting stress history to the sand – for instance by compaction – M_{DMT} increases considerably faster than q_c (see e.g. Schmertmann et al. 1986, Jendeby 1992), hence M_{DMT}/q_c increases with OCR.

The above guide provides very rough estimates of OCR. The uncertainty however may not be due necessarily to the approximate nature of the correlations. Many sands could simply not have a well defined break in their insitu *e*-log *p* curve (Fig. 14) due to the complexity of the OCR sources (cementation, desiccation, water level fluctuations, etc.). Besides, layers of sands are often stratified, as the sand layers in Fig. 11b, with OCR presumably seesawing, so that the *break* in the *e*-log *p* of the composite layer will be rounded, and assigning a unique value to OCR of the layer could be inappropriate.

Uncertainty in the values of OCR represents a problem for many models requiring a precise value of OCR in *sand* because their predictions are generally critically sensitive to OCR. For instance in the case of Venezia-Treporti mentioned before, using advanced models with OCR = 1.2 or OCR = 1.6 leads to completely different settlement predictions, while the conventional analysis using the tangent modulus M_{DMT} produced a stable and satisfactory prediction (Fig. 11c).

The cause of the advanced model sensitivity can be understood even with the simple oedometer scheme. If a sand has an in situ *e*-log *p* curve of the type in Fig. 14b, and is modeled as in Fig. 14a, the predicted settlements will be highly dependent on the choice of the abscissa of the (in reality non existing) break.

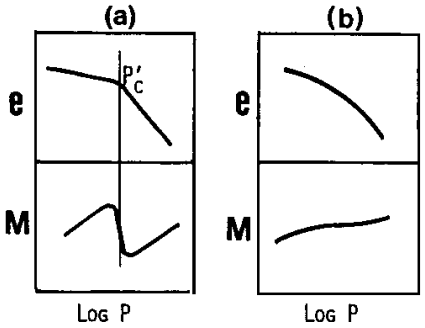

FIG. 14. Variation of *e* and *M* with *p* in presence/absence of a well defined break

Therefore *sands* whose in situ *e*-log *p* curve are of the type in Fig. 14b should probably be treated with models *attenuating* the stiffness discontinuity across the preconsolidation stress.

In short, the problem could be not so much the determination of the exact OCR in sand, but the possibly incorrect assumption of the model that the sand has a sharp break.

It is generally recommended to run both advanced and traditional analyses to avoid gross errors that are likely if one is not familiar with the details of the program. This recommendation appears appropriate in this case, because, at least in the described Venezia-Treporti case, the simplified analysis using *M* produced a stable and satisfactory prediction, while the "advanced" analysis was found to be critically dependent on the possibly elusive value of OCR.

USE OF SDMT FOR LIQUEFACTION

SDMT routinely provides, among other measurements, pairs of profiles of K_D and V_S – both correlated with the liquefaction resistance of sands. Hence SDMT permits to obtain two parallel independent estimates of liquefaction resistance CRR, one from K_D and one from V_S, using CRR-K_D and CRR-V_S correlations – where CRR is the cyclic resistance ratio, a basic input in the commonly used Seed and Idriss (1971) simplified procedure.

The use of V_S for evaluating CRR is well known. The most popular CRR-V_S correlation (Fig. 15) is the one proposed by Andrus and Stokoe (2000), modified by Andrus et al. (2004). CRR is obtained as a function of $V_{S1} = V_S \, (p_a / \sigma'_{v0})^{0.25}$, shear wave velocity corrected for the overburden stress σ'_{v0} (p_a = atmospheric pressure). The CRR-V_{S1} curves in Fig. 15 are for magnitude M_w = 7.5 earthquakes (magnitude scaling factors should be applied for different magnitudes).

Correlations CRR-K_D have been developed in the last two decades, stimulated by the recognized sensitivity of K_D to a number of factors which are known to increase liquefaction resistance, which are difficult to sense by other tests, such as stress history, prestraining, cementation, structure, and by the relationship of K_D to relative density and state parameter.

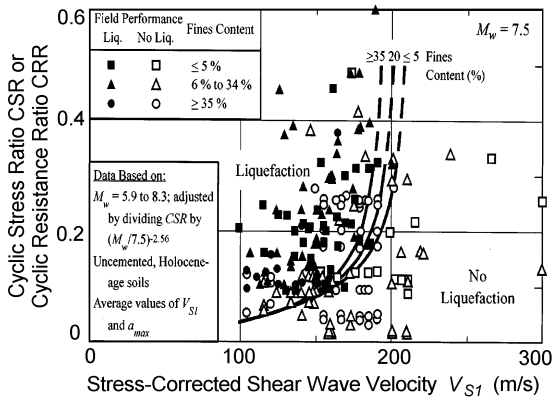

FIG. 15. Curves for evaluating CRR from V_S for clean uncemented soils (Andrus and Stokoe 2000)

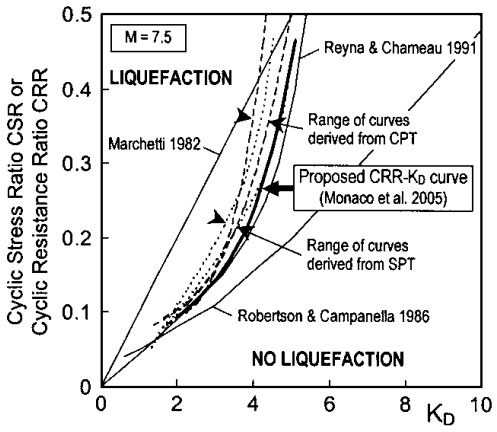

FIG. 16. Curves for evaluating CRR from K_D (Monaco et al. 2005)

A key element of the correlation CRR-K_D (Monaco and Schmertmann 2007, Monaco and Marchetti 2007) is the ability of K_D to reflect *aging* in sands. Calibration chamber data (Jamiolkowski and Lo Presti 1998) suggest that sensitivity to aging of sand is 3 to 7 times higher for K_D than for penetration resistance (see Fig. 6 in Monaco and Marchetti 2007). *Aging* in sand is a factor having a first order of magnitude influence on liquefaction behavior, as pointed out e.g. by Leon et al. (2006).

Fig. 16 summarizes the various correlations developed to estimate CRR from K_D (for magnitude M = 7.5 and clean sand) – to be used according to "simplified procedure" – including the latest CRR-K_D correlation (Monaco et al. 2005), based on all previous data.

Comparisons based on parallel measurements of K_D and V_S by SDMT at several sandy sites (Maugeri and Monaco 2006) have indicated that methods based on K_D and V_S often provide, at the same site, substantially different estimates of CRR. Generally CRR from V_S was found to be "more optimistic".

This finding opens the question "which CRR should be given greater weight", which is further discussed in the next section.

SDMT RESULTS AT VARIOUS TEST SITES

This section presents three examples of SDMT results considered of some interest.

OCR and K_D Crusts in Sand

"Crust-like" K_D profiles, very similar to the typical K_D profiles found in OC desiccation crusts in clay, have been found at the top of many sand deposits. Various indications (Maugeri and Monaco 2006) suggest that "K_D crusts" in sands reflect stress history (OCR, cementation, aging and/or other effects), rather than higher relative density. In the case shown in Fig. 17 (Catania), as in many other cases, the

existence of a shallow *"stress history crust"* (believed by far not liquefiable) is clearly highlighted by the K_D profile, but almost "unfelt" by the V_S profile. This suggests a lesser ability of V_S to profile liquefiability.

Role of the Interparticle Bonding

The SDMT profiles in Fig. 18 (Cassino) show relatively high V_S values coexisting with very low values of K_D and moduli *M*. A possible explanation: the shear wave travels fast due to the interparticle bonding (typical of many volcanic sands in this area), preserved at small strains. By contrast K_D is "low" because it reflects a different material, where the interparticle bonding has been at least partly destroyed by the DMT blade penetration. As noted by Andrus and Stokoe (2000), weak interparticle bonding can increase V_S (measured at small strains), while not necessarily increasing resistance to liquefaction, a phenomenon occurring at medium to high strains (range of K_D measurement). Thus, for liquefiability, the K_D predictions could be possibly more fitting in case of strong earthquakes. Very light earthquakes, however, may not destroy bonding, then CRR evaluated by V_S may be appropriate in this case.

Limiting "No Liquefaction" Values of V_{S1} and K_D

The vertical asymptotes of the curves CRR-V_{S1} (Fig. 15) and CRR-K_D (Fig. 16) identify limiting values of V_{S1} and K_D (roughly, for clean sand, V^*_{S1} = 215 m/s and K^*_D = 5.5) for which liquefaction can be definitely excluded for any earthquake.

At the site of the Zelazny Most dam (Fig. 19) the indications derivable from such vertical asymptotes put in evidence a clear contradiction. While the values of V_{S1} > 215 m/s suggest "no liquefaction" even in case of strong earthquakes, the values of $K_D \approx$ 1.5-2 indicate that liquefaction may occur above a certain seismic stress level (high cyclic stress ratio CSR). Even in this case, as noted before, CRR from V_S is "more optimistic" – one reason being that it partly relies on bonding or equivalent phenomena.

In the case of the Zelazny Most dam the contradiction has no practical effects, since the region is non seismic and both Fig. 15 and Fig. 16 indicate no liquefaction. But for high seismicity cases the question "which CRR should be given greater weight" remains open.

Figures 17-18-19 are also examples of a commonly noted feature: the much smoother shape of the V_S profiles compared with the *M* or K_D profiles.

SDMT INSIDE BACKFILLED BOREHOLES

In cases where the soil is too hard to penetrate (or even in rock), SDMT can be carried out inside a borehole backfilled with sand (only V_S, no DMT measurements).

The good agreement observed between V_S profiles obtained by parallel SDMT soundings carried out, at the same site, in the natural soil and in a backfilled borehole (Fig. 20) supports the reliability of V_S values obtained by this procedure.

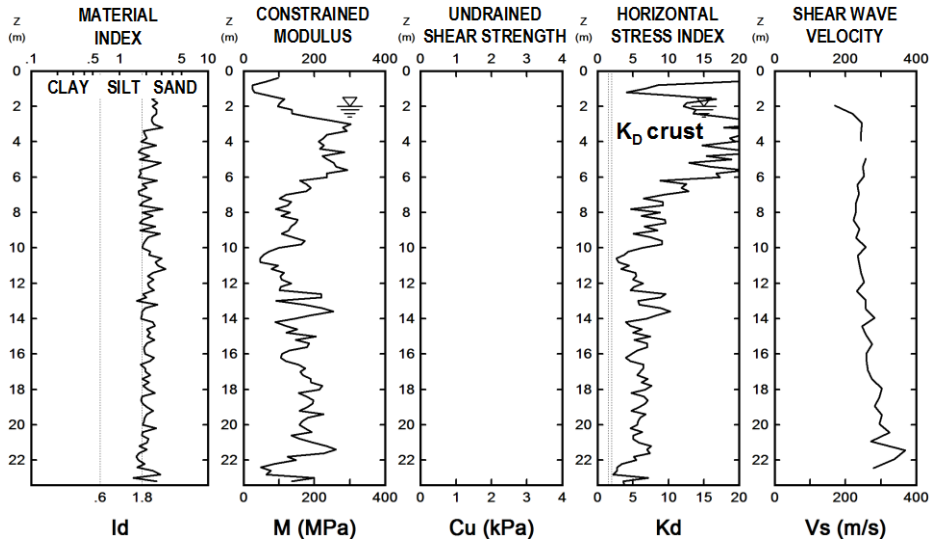

FIG. 17. SDMT profiles at the site of Catania – San Giuseppe La Rena (Italy)

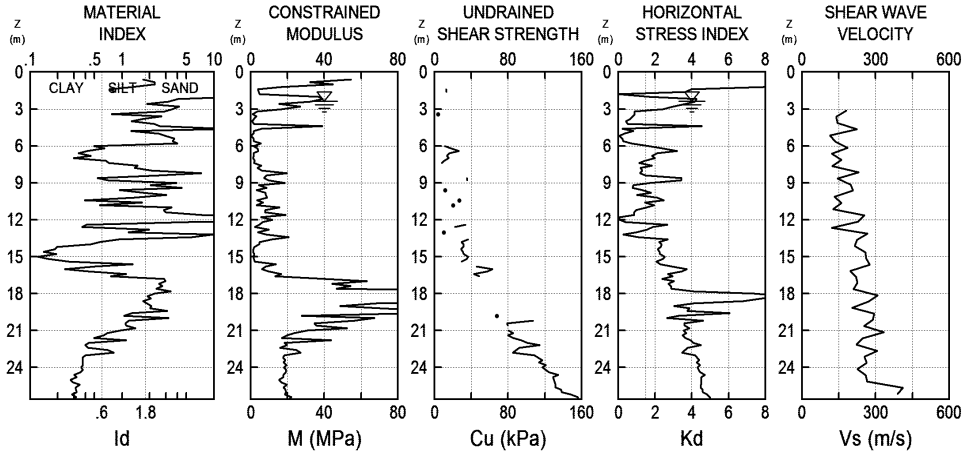

FIG. 18. SDMT profiles at the site of Cassino (Italy)

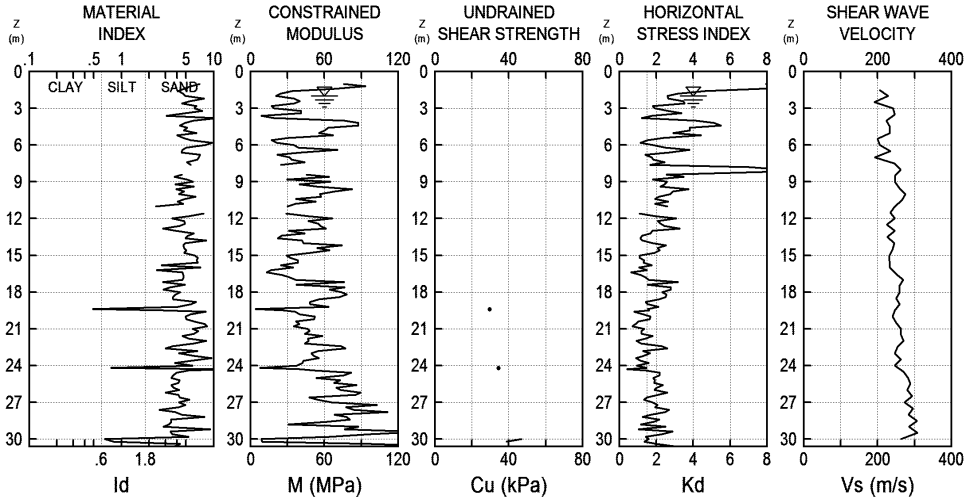

FIG. 19. SDMT profiles at the site of the Zelazny Most Tailing Dam (Poland)

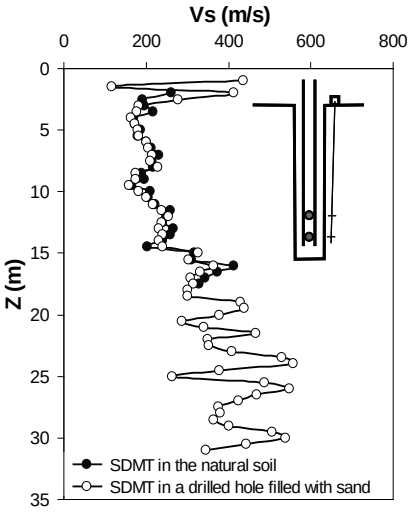

FIG. 20. Comparison of V_S profiles obtained by SDMT in the natural soil and in a backfilled borehole at the site of Montescaglioso – Ginosa (Matera), Italy

CONCLUSIONS

The seismic dilatometer (SDMT) provides accurate and highly reproducible measurements of the shear wave velocity V_S – a basic input parameter for seismic analyses. Besides V_S, SDMT provides the usual DMT results (e.g. constrained modulus M_{DMT}) for current design applications.

Based on a large number of results by SDMT, diagrams showing experimental interrelationships G_0, E_D, M_{DMT} have been constructed. In particular Fig. 9 and Fig. 10 illustrate the most significant observed trends.

Recent experience indicates that SDMT investigations can be performed with good results also in unusual conditions, e.g. *offshore* or in non penetrable soils (V_S - only measurements in backfilled boreholes).

Current research investigates the possible use of the SDMT for deriving "in situ" decay curves of soil stiffness with strain level, by fitting "reference G-γ curves" through two points provided by SDMT at different strain levels: the *small strain* shear modulus G_0 (from V_S) and a *working strain* modulus corresponding to M_{DMT}.

Deriving the operative modulus M for settlement predictions from G_0 appears arduous. Often to drastic variations in the M profile correspond barely visible variations in the G_0 profile. The ratio G_0/M varies in the wide range 0.5 to 20 (Fig. 7), hence it is far from being a constant, especially in clays and silts. Its value is strongly dependent on multiple information, e.g. soil type and stress history. Hence the use of only one information (e.g. c_u in cohesive soils) as a proxy of V_S (or G_0) for the seismic soil classification appears problematic.

If only mechanical DMT results are available rough estimates of G_0 from M can be obtained from Fig. 9.

The SDMT provides two parallel independent evaluations of the liquefaction resistance CRR from V_S and from K_D (horizontal stress index) by means of

correlations CRR-V_S (Fig. 15) and CRR-K_D (Fig. 16), to be used in the framework of the Seed and Idriss (1971) simplified procedure. Preliminary studies indicate that methods based on K_D and V_S often provide substantially different estimates of CRR. In principle, the authors would propose to give greater weight to CRR by K_D for various reasons – above all the higher sensitivity of K_D to *stress history* and *aging*, factors which greatly increase liquefaction resistance. Very light earthquakes, however, may not destroy bonding, and in that case CRR evaluated by V_S may be more appropriate. The above obviously deserves additional verification, supported by real-life liquefaction case histories.

REFERENCES

AGI (1991). "Geotechnical Characterization of Fucino Clay." *Proc. X ECSMFE*, Firenze, 1, 27-40.

Andrus, R.D. and Stokoe, K.H., II. (2000). "Liquefaction resistance of soils from shear-wave velocity." *J. Geotech. Geoenv. Engrg.*, ASCE, 126(11), 1015-1025.

Andrus, R.D., Stokoe, K.H., II and Juang, C.H. (2004). "Guide for Shear-Wave-Based Liquefaction Potential Evaluation." *Earthquake Spectra*, 20(2), 285-305.

Cunha, R.P. (2004). "Discussion Report: Applications to Geotechnical Structures." *Proc. 2nd Int. Conf. on Site Characterization ISC'2*, Porto, 2, 1391-1395.

Hepton, P. (1988). "Shear wave velocity measurements during penetration testing." *Proc. Penetration Testing in the UK*, ICE, 275-278.

Ishihara, K. (2001). "Estimate of relative density from in-situ penetration tests." *Proc. Int. Conf. on In Situ Measurement of Soil Properties and Case Histories*, Bali, 17-26.

Jamiolkowski, M. and Lo Presti, D.C.F. (1998). "DMT research in sand. What can be learned from calibration chamber tests." *1st Int. Conf. on Site Characterization ISC'98*, Atlanta. Oral presentation.

Jendeby, L. (1992). "Deep Compaction by Vibrowing." *Proc. Nordic Geotechnical Meeting NGM-92*, 1, 19-24.

Ladd, C.C. (1971). "Settlement analyses for cohesive soils." *Special Summer Program on Soft Ground Construction*, Report R71-2, Soils Publication 272.

Leon, E., Gassman, S.L. and Talwani, P. (2006). "Accounting for Soil Aging When Assessing Liquefaction Potential." *J. Geotech. Geoenv. Engrg.*, ASCE, 132(3), 363-377.

Marchetti, S. (1980). "In Situ Tests by Flat Dilatometer." *J. Geotech. Engrg. Div.*, ASCE, 106(GT3), 299-321.

Martin, G.K. and Mayne, P.W. (1997). "Seismic Flat Dilatometer Tests in Connecticut Valley Varved Clay." *ASTM Geotech. Testing J.*, 20(3), 357-361.

Martin, G.K. and Mayne, P.W. (1998). "Seismic flat dilatometer in Piedmont residual soils." *Proc. 1st Int. Conf. on Site Characterization ISC'98*, Atlanta, 2, 837-843.

Maugeri, M. and Monaco, P. (2006). "Liquefaction Potential Evaluation by SDMT." *Proc. 2nd Int. Conf. on the Flat Dilatometer*, Washington D.C., 295-305.

Mayne, P.W. (2001). "Stress-strain-strength-flow parameters from enhanced in-situ tests." *Proc. Int. Conf. on In Situ Measurement of Soil Properties and Case Histories,* Bali, 27-47.

Mayne, P.W. (2005). "Unexpected but foreseeable mat settlements of Piedmont residuum." *Int. J. of Geoengineering Case Histories,* Vol. 1, Issue 1, 5-17.

Mayne, P.W., Schneider, J.A. and Martin, G.K. (1999). "Small- and large-strain soil properties from seismic flat dilatometer tests." *Proc. 2nd Int. Symp. on Pre-Failure Deformation Characteristics of Geomaterials,* Torino, 1, 419-427.

McGillivray, A. and Mayne, P.W. (2004). "Seismic piezocone and seismic flat dilatometer tests at Treporti." *Proc. 2nd Int. Conf. on Site Characterization ISC'2,* Porto, 2, 1695-1700.

Młynarek, Z., Gogolik, S. and Marchetti, D. (2006). "Suitability of the SDMT method to assess geotechnical parameters of post-flotation sediments." *Proc. 2nd Int. Conf. on the Flat Dilatometer,* Washington D.C., 148-153.

Monaco, P. and Marchetti, S. (2007). "Evaluating liquefaction potential by seismic dilatometer (SDMT) accounting for aging/stress history." *Proc. 4th Int. Conf. on Earthquake Geotechnical Engineering ICEGE,* Thessaloniki.

Monaco, P., Marchetti, S., Totani, G. and Calabrese, M. (2005). "Sand liquefiability assessment by Flat Dilatometer Test (DMT)." *Proc. XVI ICSMGE,* Osaka, 4, 2693-2697.

Monaco, P. and Schmertmann, J.H. (2007). Discussion of "Accounting for Soil Aging When Assessing Liquefaction Potential" by Leon, E. et al. (in *J. Geotech. Geoenv. Engrg.*, ASCE, 2006, 132(3), 363-377). *J. Geotech. Geoenv. Engrg.*, ASCE, 133(9), 1177-1179.

Monaco, P., Totani, G. and Calabrese, M. (2006). "DMT-predicted vs observed settlements: a review of the available experience." *Proc. 2nd Int. Conf. on the Flat Dilatometer,* Washington D.C., 244-252.

Powell, J.J.M. and Butcher, A.P. (2004). "Small Strain Stiffness Assessments from in Situ Tests." *Proc. 2nd Int. Conf. on Site Characterization ISC'2,* Porto, 2, 1717-1722.

Schmertmann, J.H. (1986). "Dilatometer to compute Foundation Settlement." *Proc. ASCE Spec. Conf. on Use of In Situ Tests in Geotechnical Engineering In Situ '86,* Virginia Tech, Blacksburg. ASCE Geotech. Spec. Publ. No. 6, 303-321.

Schmertmann, J.H., Baker, W., Gupta, R. and Kessler, K. (1986). "CPT/DMT Quality Control of Ground Modification at a Power Plant." *Proc. ASCE Spec. Conf. on Use of In Situ Tests in Geotechnical Engineering In Situ '86,* Virginia Tech, Blacksburg. ASCE Geotech. Spec. Publ. No. 6, 985-1001.

Seed, H.B. and Idriss, I.M. (1971). "Simplified procedure for evaluating soil liquefaction potential." *J. Geotech. Engrg. Div.,* ASCE, 97(9), 1249-1273.

Simpson, B. (1999). "Engineering needs." *Proc. 2nd Int. Symp. Pre-Failure Deformation Characteristics of Geomaterials,* Torino.

TC16 (2001). "The Flat Dilatometer Test (DMT) in Soil Investigations - A Report by the ISSMGE Committee TC16." May 2001, 41 pp. Reprinted in *Proc. 2nd Int. Conf. on the Flat Dilatometer,* Washington D.C., 7-48.

Terzaghi, K. and Peck, R.B. (1964). "Soil Mechanics in Engineering Practice." John Wiley & Sons.0